Warsztaty metod fizycznych w medycynie

26.02.2020 - zajęcia nr 1

Warsztaty metod fizycznych w medycynie

- Szczegóły organizacyjne
- Rozkład jazdy
- Zasady zaliczania
- Podstawy prezentacji naukowej

Szczegóły organizacyjne

- Środy 10:15 - 12:00, obecność obowiązkowa
- 5 wizyt w jednostkach naukowych i klinicznych (nie tylko diagnostyka)
- Strona przedmiotu: http://www.fuw.edu.pl/~bbrzozow/FizMed/WzMD/WzMD.html —> logowanie

login: fizykmedyczny
hasło: czydzialahaslo

Rozkład jazdy

Wykład i dyskusja + Zwiedzanie + Referaty

zaproszony ekspert

lista publikacji

Program przedmiotu

Data	Blok	Zajęcia
4 marca	radiobiologia	wykład: dr Maria Kowalska, 10:15
9 marca	radiobiologia	IChTJ, 9:30
18 marca	radiobiologia	referaty
23 marca	stomatologia	wykład: Paweł Roszkiewicz, 9:30 wizyta w Laskach
1 kwietnia	stomatologia	referaty
15 kwietnia	medycyna nuklearna	wykład: dr Adam Bajera, 10:15
20 kwietnia	medycyna nuklearna	Szpital na Banacha, 9:30
29 kwietnia	medycyna nuklearna	referaty
6 maja	radioterapia	wykład: dr Anna Zawadzka, 10:15
11 maja	radioterapia	NIO, 10:45
20 maja	radioterapia	referaty
27 maja	obrazowanie	wykład: Witold Skrzyński, 10:15
1 czerwca	obrazowanie	Szpital MSWiA, 9:30
10 czerwca	obrazowanie	referaty

Zasady zaliczenia

1. Obecność podczas wizyt (0 - 10 pkt)

- możliwe dwie nieusprawiedliwione nieobecności na zajęciach

2. Wygłoszenie 5 referatów (0 - 30 pkt)

- uśredniona liczba punktów ze wszystkich prezentacji (15 min + 5 min)

3. Zadawanie pytań (0 - 5 pkt)

Referaty

1. Lista 9 tematów będzie pojawiała się najpóźniej tydzień przed zajęciami na stronie przedmiotu (rezerwacja online plus mail: adrianna.tartas@fuw.edu.pl).

- oprócz publikacji referencyjnej należy znaleźć inne materiały źródłowe

2. Ocena prezentacji na podstawie poniższych kryteriów:

Oceniane elementy prezentacji	**Liczba punktów**
Zgodność z tematem	0 - 2
Poziom merytoryczny	0 - 8
Poprawność językowa	0 - 5
Estetyka wykonanej pracy	0 - 5
Odpowiednie tempo prezentacji	0 - 2
Uporządkowany i logiczny układ prezentacji	0 - 4
Dbałość o zainteresowanie odbiorców	0 - 4

Kartki z notatkami są zabronione!

3. Prezentacje muszą byc wysłane do koordynatora przedmiotu (AT) najpóźniej godzinę przed rozpoczęciem zajęć (09:15).

Jak czytać publikację?

- Imaging quality of 44Sc in comparison with five other PET radionuclides using Darenzo phantoms and preclinical PET
- Initial events in the cellular effects of ionizing radiations: clustered damage in DNA

Applied Radiation and Isotopes 110 (2016) 129–133

Contents lists available at ScienceDirect

Applied Radiation and Isotopes

journal homepage: www.elsevier.com/locate/apradiso

Technical note

Imaging quality of ^{44}Sc in comparison with five other PET radionuclides using Derenzo phantoms and preclinical PET

Maruta Bunka [a,b,1], Cristina Müller [c,*,1], Christiaan Vermeulen [c], Stephanie Haller [c], Andreas Türler [a,b], Roger Schibli [c,d], Nicholas P. van der Meulen [a,c,*]

[a] Laboratory of Radiochemistry and Environmental Chemistry, Paul Scherrer Institute, Villigen-PSI, Switzerland
[b] Laboratory of Radiochemistry and Environmental Chemistry, Department of Chemistry and Biochemistry University of Bern, Bern, Switzerland
[c] Center for Radiopharmaceutical Sciences ETH-PSI-USZ, Paul Scherrer Institute, Villigen-PSI, Switzerland
[d] Department of Chemistry and Applied Biosciences, ETH Zurich, Zurich, Switzerland

HIGHLIGHTS

- Six PET radionuclides (^{18}F, ^{64}Cu, ^{11}C, ^{89}Zr, ^{68}Ga and ^{44}Sc) were produced at CRS ETH-PSI-USZ.
- Preclinical PET was performed with Derenzo phantoms.
- The FWHM values was determined for each radionuclide with the same preclinical PET scanner.
- In agreement with decreasing positron energies, the image resolution increased: ^{68}Ga < ^{44}Sc < ^{89}Zr < ^{11}C < ^{64}Cu < ^{18}F.
- The FWHM of the radionuclides, were in agreement with the theoretical predictions of Palmer et al. (2005).

Applied Radiation and Isotopes 110 (2016) 129–133

Contents lists available at ScienceDirect

Applied Radiation and Isotopes

journal homepage: www.elsevier.com/locate/apradiso

Technical note

Imaging quality of ^{44}Sc in comparison with five other PET radionuclides using Derenzo phantoms and preclinical PET

Maruta Bunka [a,b,1], Cristina Müller [c,*,1], Christiaan Vermeulen [c], Stephanie Haller [c], Andreas Türler [a,b], Roger Schibli [c,d], Nicholas P. van der Meulen [a,c,*]

[a] Laboratory of Radiochemistry and Environmental Chemistry, Paul Scherrer Institute, Villigen-PSI, Switzerland
[b] Laboratory of Radiochemistry and Environmental Chemistry, Department of Chemistry and Biochemistry University of Bern, Bern, Switzerland
[c] Center for Radiopharmaceutical Sciences ETH-PSI-USZ, Paul Scherrer Institute, Villigen-PSI, Switzerland
[d] Department of Chemistry and Applied Biosciences, ETH Zurich, Zurich, Switzerland

HIGHLIGHTS

- Six PET radionuclides (^{18}F, ^{64}Cu, ^{11}C, ^{89}Zr, ^{68}Ga and ^{44}Sc) were produced at CRS ETH-PSI-USZ.
- Preclinical PET was performed with Derenzo phantoms.
- The FWHM values was determined for each radionuclide with the same preclinical PET scanner.
- In agreement with decreasing positron energies, the image resolution increased: ^{68}Ga < ^{44}Sc < ^{89}Zr < ^{11}C < ^{64}Cu < ^{18}F.
- The FWHM of the radionuclides, were in agreement with the theoretical predictions of Palmer et al. (2005).

ARTICLE INFO

Article history:
Received 24 October 2015
Received in revised form
28 November 2015
Accepted 5 January 2016
Available online 6 January 2016

Keywords:
PET
^{18}F
^{64}Cu
^{11}C
^{89}Zr
^{44}Sc
^{68}Ga
Phantom
Resolution

ABSTRACT

PET is the favored nuclear imaging technique because of the high sensitivity and resolution it provides, as well as the possibility for quantification of accumulated radioactivity. ^{44}Sc ($T_{1/2}$=3.97 h, Eβ^+=632 keV) was recently proposed as a potentially interesting radionuclide for PET. The aim of this study was to investigate the image quality, which can be obtained with ^{44}Sc, and compare it with five other, frequently employed PET nuclides using Derenzo phantoms and a small-animal PET scanner. The radionuclides were produced at the medical cyclotron at CRS, ETH Zurich (^{11}C, ^{18}F), at the Injector II research cyclotron at CRS, PSI (^{64}Cu, ^{89}Zr, ^{44}Sc), as well as via a generator system (^{68}Ga). Derenzo phantoms, containing solutions of each of these radionuclides, were scanned using a GE Healthcare eXplore VISTA small-animal PET scanner. The image resolution was determined for each nuclide by analysis of the intensity signal using the reconstructed PET data of a hole diameter of 1.3 mm. The image quality of ^{44}Sc was compared to five frequently-used PET radionuclides. In agreement with the positron range, an increasing relative resolution was determined in the sequence of ^{68}Ga < ^{44}Sc < ^{89}Zr < ^{11}C < ^{64}Cu < ^{18}F. The performance of ^{44}Sc was in agreement with the theoretical expectations based on the energy of the emitted positrons.

1. Introduction

Current clinical PET is the favored method of nuclear physicians because of the high sensitivity and resolution it provides, as well as the possibility for quantification of accumulated radioactivity (Mittra and Quon, 2009; Rahmim and Zaidi, 2008). The resolution of the reconstructed image is mainly dependent on (i) detector-specific effects, (ii) photon non-collinearity and the (iii) positron range of the employed PET nuclide (Rahmim and Zaidi, 2008). Detector-specific effects (e.g. size and geometry) are dependent on the type of PET scanner employed. Non-collinearity originates from the fact that the two 511 keV photons are not emitted precisely in opposite (180°-angle) directions. The corresponding resolution blurring depends on the ring diameter and is, therefore, of minor importance in the case of small-animal PET, but may be of relevance for clinical PET (Rahmim and Zaidi, 2008). The third factor is the positron range, defined as the average direct distance

* Corresponding authors at: Center for Radiopharmaceutical Sciences ETH/PSI/USZ and Laboratory of Radiochemistry, Paul Scherrer Institute, 5232 Villigen-PSI, Switzerland.
E-mail addresses: cristina.mueller@psi.ch (C. Müller), nick.vandermeulen@psi.ch (N.P. van der Meulen).
[1] Contributed equally to this manuscript.

http://dx.doi.org/10.1016/j.apradiso.2016.01.006
0969-8043/

cancer and inflammatory diseases (Basu and Alavi, 2008). In recent times, positron-emitting radiometals have also been increasingly introduced in clinical practice (Kramer-Marek and Capala, 2012; Laforest and Liu, 2008). ^{68}Ga is obtained from a ^{68}Ge/^{68}Ga generator and, due to its short half-life, it is suitable mainly for the labeling of small molecules and peptides with fast pharmacokinetics (Table 1) (Eiber et al., 2015; Gabriel et al., 2007). Other interesting cyclotron-produced radiometals are ^{64}Cu and ^{89}Zr, which have been widely used pre-clinically, as well as in clinics (Table 1) (Anderson and Ferdani, 2009; Dijkers et al., 2010).

More recently, ^{44}Sc has attracted the attention of researchers and physicians because of its excellent characteristics for PET imaging (Table 1) (Roesch, 2012). The production of ^{44}Sc has been proposed via a ^{44}Ti/^{44}Sc-generator (Roesch, 2012) or by irradiation of natural or enriched Ca targets at a cyclotron (Krajewski et al., 2013; Müller et al., 2013; Severin et al., 2012). It has been recently demonstrated that cyclotron-produced ^{44}Sc can be made available in sufficient quantities for clinical application (van der Meulen et al., 2015). ^{44}Sc may, therefore, be an attractive alternative to the currently-used ^{68}Ga due to its almost four-fold longer half-life which allows transportation of ^{44}Sc-radiopharmaceuticals to hospitals remote from PET centers containing a cyclotron (van der Meulen et al., 2015).

While ^{11}C, ^{18}F, ^{64}Cu and ^{89}Zr have been investigated and compared in detail by Palmer et al. (2005), the question remains how ^{44}Sc fits into the sequence of these radionuclides in terms of imaging resolution. In the present study, five common PET nuclides (^{11}C, ^{18}F, ^{68}Ga, ^{64}Cu and ^{89}Zr) were investigated with regard to their relative image resolution using small-animal PET for comparison with the results obtained with ^{44}Sc. For this purpose, Derenzo phantoms were used, along with a GE Healthcare eXplore Vista small-animal PET scanner.

2. Experimental arrangement

2.1. Production of ^{18}F, ^{11}C, ^{68}Ga, ^{64}Cu, ^{89}Zr

No-carrier-added [^{18}F]fluorine was produced via the ^{18}O(p,n)^{18}F nuclear reaction by irradiation of enriched ^{18}O-water at a Cyclone 18/9 cyclotron (18 MeV; IBA, Ottignies-Louvain-la-Neuve, Belgium) was determined in dose calibrators (ISOMED 2010, Nuclear-Medizintechnik, Dresden GmbH or VDC-505, Veenstra Instruments, The Netherlands). The factors for non-standard nuclides, such as for instance ^{44}Sc, were determined based on exact activity measurements on a N-type high-purity germanium (HPGe) coaxial detector (EURISYSMESURES, France) using *Ortec InterWinner* software version 5.0.

The radionuclidic purity of all investigated radionuclides was $>99\%$. ^{44}Sc comprised traces of ^{44m}Sc ($<1\%$) (Müller et al., 2013) and ^{88}Zr ($<1\%$) was present as a radionuclidic impurity in the ^{89}Zr solution (Hohn et al., 2008).

2.2. Preparation of the phantoms

Derenzo phantoms with a diameter of $D=19.5$ mm, a height of $H=15.0$ mm and holes with diameters ranging from 0.8 mm to 1.3 mm in 0.1 mm steps were used for this study (Supplementary material Fig. S1). The phantoms were filled (total volume of 600 μL) with the aqueous solution of the desired nuclide and ethanol (25 vol%) to enable proper filling of the capillaries.

2.3. PET imaging

All PET scans were performed with the same preclinical scanner, a small-animal eXplore VISTA PET/CT (GE Healthcare, Spain) at an energy window of 250–700 keV. The features and characteristics of this kind of preclinical PET scanner have been reported in detail by Wang et al. (2006). Based on the measured count rate (counts/s) of each radionuclide, the required scan time for ~60 Mio coincidences was determined. The 2-dimensional ordered-subset expectation maximization (2D-OSEM) algorithm was used for the reconstruction of the PET data and the images were prepared using *VivoQuant* image post-processing program software (version 2.00, Bioscan Inc., U.S.).

2.4. Quantification of the relative resolution by determination of full-width at half-maximum (FWHM)

With the "cropping" function of the *VivoQuant* software, one representative single transversal section was selected at three different depths of the phantom. A line was drawn through the

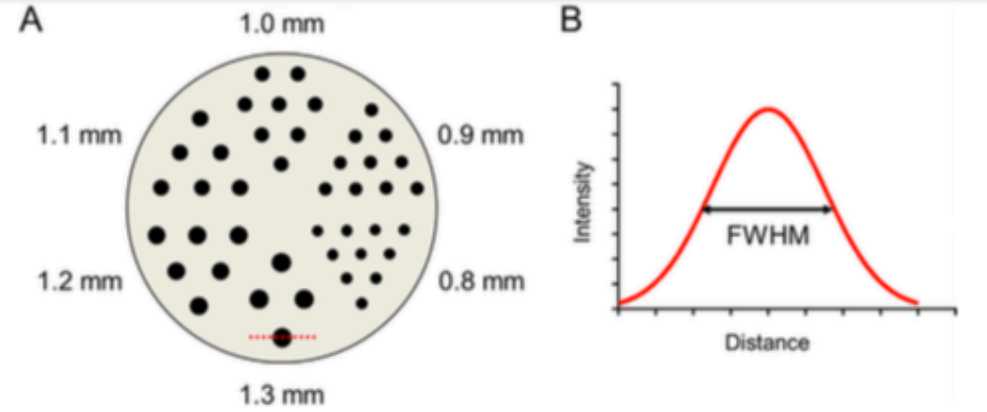

Fig. 1. (A) Scheme of the hole alignment of the Derenzo phantom. The 1.3 mm hole which was used for determination of the full-width at half-maximum (FWHM) is indicated in red. (B) Cubic spline fitted for the intensity curve of the 1.3 mm hole to allow determination of the FWHM. (For interpretation of the references to color in this figure legend, the reader is referred to the web version of this article.)

center point of the radioactive spot obtained from the 1.3 mm-hole of the Derenzo phantom (Fig. 1A) and then the "distance/annotation" function of the *VivoQuant* software was applied to produce an intensity plot of the selected profile. The plot data were saved as a *csv*-file for export. The data were transferred to *Origin 2015*, which allowed normalization by background subtraction. More specifically, this means that the intensity plot line was drawn from dark-to-dark and the lowest value of the start and end points was set to zero. A cubic spline was then fitted through the data and the full-width at half-maximum (FWHM) was determined (Fig. 1B). The listed values in Table 2 indicate the average and standard deviation of 3 determinations for FWHM based on the 3 different sections of each phantom scan. One section of each phantom scan is shown in Fig. 2. In order to obtain an optimal image, the intensity of the color scale was adjusted manually.

3. Results and discussion

3.1. Theoretical spatial resolution

Spatial resolution is a parameter describing the system's ability to distinguish between two radioactive sources in an image. In theory, this parameter is expressed as the full-width at half-maximum (FWHM) and is specific for a particular PET system (Palmer et al., 2005). For this study, scanner-specific parameters refer to the eXplore VISTA PET scanner which was used for all phantom scans (Wang et al., 2006). The main remaining parameter responsible for the spatial resolution of a PET image is the positron range, which is dependent on the positron energy (Rahmim and Zaidi, 2008). Small positron energy results in an improved image quality, whereas high positron energy will degrade the spatial resolution, especially in small-animal PET imaging (Liu and Laforest, 2009). Given that the 1.3 mm diameter spot of the Derenzo phantom is not necessarily a *bona fide* point source in terms of the small scanner diameter, only a relative resolution assessment can be made, with a sequence expectation of increasing resolution of $^{68}Ga < ^{89}Zr < ^{11}C < ^{64}Cu < ^{18}F$, with ^{44}Sc expected to be placed between ^{68}Ga and ^{89}Zr.

Table 2
Full-width at half-maximum (FWHM) published by Palmer et al. and values determined for phantom hole-diameters of 1.3 mm for each radionuclide from 3 different sections of the PET scan.

Radionuclide	$E\beta^+_{average}$ [keV] (nudat)	FWHM [mm] (Palmer et al., 2005)	FWHM [mm] This work
^{18}F	250	1.67	1.67 ± 0.02
^{64}Cu	278	1.71	1.72 ± 0.03
^{11}C	386	1.88	1.80 ± 0.00
^{89}Zr	396	1.91	1.98 ± 0.05
^{44}Sc	**632**	**n.d.**	**2.30 ± 0.12**
^{68}Ga	830	2.74	2.48 ± 0.22

3.2. PET scans of the phantoms

In order to allow comparison of the PET image quality obtained with ^{11}C, ^{18}F, ^{64}Cu, ^{89}Zr, ^{44}Sc and ^{68}Ga the phantoms were scanned for the required time period (6–30 min) to acquire ~60 Mio coincidences (range from 49 to 65 Mio) (Table S1, Supplementary material).

3.3. Comparison of the PET image quality obtained with different nuclides

The PET images of the Derenzo phantoms obtained with each radionuclide are shown in Fig. 2. Visual comparison of the PET images revealed the best resolution for ^{18}F and ^{64}Cu, followed by ^{11}C and ^{89}Zr and ^{68}Ga, which showed clearly lower resolution. From a visual perspective, the resolution obtained with ^{44}Sc was between ^{68}Ga and ^{89}Zr. Determination of FWHM values for ^{18}F, ^{64}Cu, ^{11}C, ^{89}Zr and ^{68}Ga for a hole-diameter of 1.3 mm revealed values which were in excellent agreement with the results previously predicted by theoretical calculations of Palmer et al. (2005). In this study, the sequence of resolutions was determined with ^{18}F on top, followed by ^{64}Cu, ^{89}Zr, ^{11}C and ^{68}Ga (Table 2). The value for ^{44}Sc which has not been investigated previously revealed a resolution between those of ^{68}Ga and ^{89}Zr. The visual findings and the determined value for the FWHM of ^{44}Sc are in agreement with the expectations according to the positron energies of ^{44}Sc and the tested radionuclides, resulting in $^{18}F > ^{64}Cu > ^{11}C > ^{89}Zr > ^{44}Sc > ^{68}Ga$.

4. Conclusion

This phantom study enabled the determination of the preclinical PET imaging resolution for ^{44}Sc in comparison with five frequently-used PET radionuclides. In agreement with decreasing positron energies, we found an increasing image resolution in the sequence of $^{68}Ga < ^{44}Sc < ^{89}Zr < ^{11}C < ^{64}Cu < ^{18}F$. This study allowed visual presentation of the imaging characteristics of ^{44}Sc as it would be theoretically expected, based on its decay properties. Importantly, the experimental values for the FWHM of the investigated radionuclides were in excellent agreement with the theoretical predictions of Palmer et al. (2005).

Acknowledgments

The authors thank Walter Hirzel (PSI), Alexander Sommerhalder (PSI), Martin Hungerbühler (PSI), Dr. Linjing Mu (USZ), Dr. Thomas Betzel (ETH), Bruno Mancosu (ETH), Lukas Dialer (ETH), Martina Dragic (ETH) and Claudia Keller (ETH) for technical assistance. The research was financially supported by the Swiss National Science Foundation (PZ00P3_138834) and the Swiss Cancer League (KLS-02762-02-2011).

Appendix A. Supplementary material

Supplementary data associated with this article can be found in the online version at http://dx.doi.org/10.1016/j.apradiso.2016.01.006.

References

Anderson, C.J., Ferdani, R., 2009. Copper-64 radiopharmaceuticals for PET imaging of cancer: advances in preclinical and clinical research. Cancer Biother. Radiopharm. 24, 379–393.

Basu, S., Alavi, A., 2008. Unparalleled contribution of ^{18}F-FDG PET to medicine over 3 decades. J. Nucl. Med. 49 (17N-21N), 37N.

Dijkers, E.C., Oude Munnink, T.H., Kosterink, J.G., Brouwers, A.H., Jager, P.L., de Jong, J.R., van Dongen, G.A., Schroder, C.P., Lub-de Hooge, M.N., de Vries, E.G., 2010. Biodistribution of ^{89}Zr-trastuzumab and PET imaging of HER2-positive lesions

M. Bunka et al. / Applied Radiation and Isotopes 110 (2016) 129–133

et alli (and others)

Initial events in the cellular effects of ionizing radiations: clustered damage in DNA